J Mater Sci: Mater Med (2011) 22:2537–2543
DOI 10.1007/s10856-011-4428-y

An X-ray micro-fluorescence study to investigate the distribution of Al, Si, P and Ca ions in the surrounding soft tissue after implantation of a calcium phosphate-mullite ceramic composite in a rabbit animal model

Richard A. Martin · Zahira Jaffer · Garima Tripathi · Shekhar Nath · Mira Mohanty · Victoria FitzGerald · Pierre Lagarde · Anne-Marie Flank · Artemis Stamboulis · Bikramjit Basu

Received: 12 May 2011 / Accepted: 18 August 2011 / Published online: 30 August 2011

Abstract Synthetic calcium phosphates, despite their bioactivity, are brittle. Calcium phosphate- mullite composites have been suggested as potential dental and bone replacement materials which exhibit increased toughness. Aluminium, present in mullite, has however been linked to bone demineralisation and neurotoxicity: it is therefore important to characterise the materials fully in order to understand their in vivo behaviour. The present work reports the compositional mapping of the interfacial region of a calcium phosphate—20 wt% mullite biocomposite/soft tissue interface, obtained from the samples implanted into the long bones of healthy rabbits according to standard protocols (ISO-10993) for up to 12 weeks. X-ray micro-fluorescence was used to map simultaneously the distribution of Al, P, Si and Ca across the ceramic–soft tissue interface. A well defined and sharp interface region was present between the ceramic and the surrounding soft tissue for each time period examined. The concentration of Al in the surrounding tissue was found to fall by two orders of magnitude, to the background level, within ~35 μm of the implanted ceramic.

R. A. Martin (✉)
School of Engineering & Applied Sciences and Aston Research Centre for Healthy Ageing, University of Aston, Aston Triangle, Birmingham B4 7ET, UK
e-mail: R.A.Martin@Aston.ac.uk

Z. Jaffer · A. Stamboulis
Department of Metallurgy and Materials, University of Birmingham, Edgbaston, Birmingham B15 2TT, UK

G. Tripathi · S. Nath · B. Basu
Laboratory for Biomaterials, Department of Materials Science and Engineering, Indian Institute of Technology, Kanpur, Uttar Pradesh, India

M. Mohanty
Division of Implant Biology, BMT Wing, Sree Chitra Tirunal Institute for Medical Science and Technology, Trivandrum, Kerala, India

V. FitzGerald
School of Physical Sciences, University of Kent, Canterbury, Kent CT2 7NH, UK

P. Lagarde · A.-M. Flank
Synchrotron Soleil, L'Orme des Merisiers, BP 48, 91192 Gif/Yvette, France

1 Introduction

The mineral component of bone and teeth are formed of hydroxyapatite (HA, $Ca_{10}(PO_4)_6OH_2$). Consequently, biocompatible ceramics formed of HA have received considerable interest as potential bone replacement materials. However, pure synthetic HA is extremely brittle (fracture toughness: 0.6–1 MPa $m^{0.5}$) [1, 2]. To overcome this problem, researchers have attempted to synthesize HA and other calcium phosphate (CaP)-based composite materials, which have a better combination of physical properties than monolithic HA [2–7]. Crystalline aluminium oxide, also referred to as corundum, is one of the hardest materials known, scoring 9 on the Mohs scale of mineral hardness [8], and may therefore be added to improve the toughness and chemical durability of glasses and glass ceramics [9, 10]. We have recently developed a range of hydroxyapatite-mullite composites and calcium phosphate-mullite composites [11–13] with a view to addressing this issue. Mullite is a solid solution of aluminium oxide (alumina, Al_2O_3) and silica (SiO_2). The general formula for mullite solid solution is $Al_{(4+2x)}Si_{(2-2x)}O_{(10-x)}$, where x = 0.17 to 0.59. In the present case the formula for the mullite phase described herein is $3Al_2O_3.2SiO_2$ (i.e. x = 0.25). The present work

investigates a calcium phosphate–mullite composite prepared from 80 wt% hydroxyapatite, $Ca_{10}(PO_4)_6(OH)_2$, and 20 wt% mullite (where x = 0.25) powder. During the sintering process the hydroxyapatite decomposed to form tricalcium phosphate (TCP) which is more soluble and the composite is therefore denoted as CaP-20 wt% mullite.

In vitro and in vivo testing have shown that CaP-20 wt% mullite composites have excellent biocompatibility [11, 12]. For example, during early stage of implantation (1 week) trabeculae of newly woven bone could be observed at the host neobone-implant interface along with a cellular infiltrate of macrophages and fibroblasts. After 4 weeks, new bone was observed with the formation of Haversian canals and after 12 weeks of implantation foci of chondrocytes and remodelling of Haversian canals could be observed. The absence of any extended cavities between the bone and implant essentially reveals the integrity of the implant with host bone [11]. However, in view of the presence of mullite, it is essential to investigate any potential leaching of Al into the surrounding tissue. Studies have shown that aluminium can accumulate in the brain, muscle, liver and bone, and aluminium has been linked to bone demineralisation and neurotoxicity [14–17]. It is reported that aluminium ions can stimulate the osteoblast proliferation and thereby influence bone metabolism [18]. Aluminium ions are known to leach into the surrounding tissues from certain biomedical implants e.g. calcium aluminium sodium fluorosilicates [19]. There have been several case studies where bone cements containing aluminium have been directly attributed to patient fatality [20–22]. Consequently, there has been considerable effort to develop aluminium-free or non-leaching aluminium cements [23]. Blades et al. developed glass–ionomer cements with low/no aluminium release from the unset cement dough [24]. The release of aluminium from the set cement is reported to inhibit mineralization of osteoid and remineralisation of bone [24]. Aluminium is found in both blood cells and blood plasma and can therefore be redistributed throughout the body [14].

The European Food Safety Authority [25] and the joint Food and Agriculture Organisation of the United Nations and the World Health Organisation [26] both suggest a tolerable weekly intake of just 1 mg of aluminium per kg of body weight. However, the absorbed level of Al within the body is significantly lower since the vast majority of this aluminium passes straight through the body [27, 28]. Typical daily exposures to aluminium are tabulated in the work of Yokel and McNamara [14]. They estimate that we intake 5-10 mg of aluminium per day in our diet, although only 0.1–0.3% of this is actually absorbed into the body. They estimate the total weekly Al absorbed from normal sources (diet, air, vaccines, and antiperspirants) is *only* between 1.8 and 7 μg/kg. The estimated percentage absorbed is typically a fraction of a percentage as discussed, however for vaccines the absorption is 100% [14, 29]. Furthermore, the excretion of absorbed Al is very slow. For example, 28 days after receiving a single injection of aluminium hydroxide the cumulative excretion of Al was only 6% for New Zealand white rabbits [29].

Bone turnover (remodelling) rates in adults are low (about 3% per year for compact bone and 20% per year for cancellous or spongy bone) [16]. Consequently, aluminium has a long effective retention half-life in the skeleton, typically 10–20 years. For a 1 cm^3 implant being completely resorbed over a 5 year period (based on the 20% remodelling per year), the weekly exposure to aluminium may be calculated using the density and composition of the sintered ceramic. This yields an Al content corresponding to 0.24 g per cm^3. The resultant dissolution could therefore result in up to 0.9 mg of aluminium being absorbed per week. The implant could therefore potentially increase the normal amount of Al absorbed by over 100 times. This is particularly important given that patient fatalities have been recorded due to relatively low levels of aluminium being present. For example, following the implantation of an Al containing cement elevated levels of 9.3 μg/g (compared to normal range of 2 μg/g) of Al were found in the cortex and subcortex regions. This elevation was directly attributed to the patients seizures, dialysis associated encephalopathy and ultimate fatality [22]. The low excretion rate combined with the potential continuous release of Al from the implant could potentially result in lethal quantities of Al building up. It is therefore essential to determine if Al leaches out of the sample into the surrounding soft tissue. Given the complex chemistry of the in vivo environment, it is however difficult to predict the in vivo from in vitro observations.

Aluminium is difficult to detect using fluorescence techniques due to the low energies or 'soft' X-rays required to excite aluminium. The soft X-rays are easily absorbed and even a 30 cm path-length of air will absorb 90% of the incident beam. However it is now possible to detect aluminium at the pico-gram level by using advanced X-ray micro-fluorescence techniques. The present study investigates calcium phosphate-mullites which have already been shown to promote bone regeneration [11]. Previous studies have focussed on the ceramic/hard tissue (bone) interface to determine the ability to promote bone regeneration. This paper focuses exclusively on the ceramic/soft tissue interface. We present the results of X-ray fluorescence measurements undertaken to investigate the potential movement of Al ions into the peri-implant tissue after in vivo testing and as a function of implantation time (up to 12 weeks). In addition, co-mapping was performed between Al, Si, P and Ca across the bioceramic soft tissue interface after in vivo testing.

2 Methods

2.1 Preparation of the ceramic implant

CaP-mullite composites were prepared by sintering a mixture of HA and mullite powders. HA was first synthesized using the suspension precipitation route [30] whilst commercially procured mullite (KCM Corporation, Japan) with an average particle size of 1.04 μm was used. The powders were mixed in a ratio of 80 wt% HA:20 wt% mullite and ground using a ball mill (wet milling) for 16 h to obtain a fine homogeneously mixed composite powder mixture. The mixture was then pressed and subsequently sintered for 2 h at 1350°C. The resulting cylindrical samples were 2 ± 0.05 mm in diameter and 6 mm in length.

2.2 Surgical procedure

The sintered CaP-20% mullite ceramic samples, after ultrasonication and sterilization, were implanted in the rabbit model for three different time periods of 1, 4 and 12 weeks, and the entire implantation protocol followed the ISO-10993 guidelines. During the implantation, 2 mm sized holes were made in the femurs of the rabbits and the bioceramic composite samples were placed in those holes. Subsequently, the wound was closed using stitches. All the animals were given postoperative care after the surgical procedure. X-ray radiography observations of the implantation sites did not reveal any evidence of tissue reaction. After the desired period (1, 4 and 12 weeks) of implantation, the femur bones with the bioceramic composite implant materials were removed and fixed in 10% buffered formalin. Further details of the histopathological procedure are given by Nath et al. [11].

2.3 Sample preparation

After fixation, a cross section of each implant with surrounding soft tissue was cut using a high precision diamond saw. The tissue samples were embedded in poly methyl methacrylate (PMMA). Thin sections (100–150 μm) of the resultant resin blocks were cut and polished. Thin sample sections across the ceramic/soft tissue interface were investigated using X-ray micro-fluorescence.

2.4 Fluorescence mapping

Fluorescence measurements were undertaken on the LUCIA beam line at the Soleil synchrotron radiation facility [31, 32] using an incident energy of 4.1 keV. The incident beam was focused to give a 5 μm × 5 μm spot size. The fluorescence spectra were divided into the four regions of interest enabling Al, Si, P and Ca to be mapped simultaneously. Each energy region was integrated to give the total counts detected per element. All measurements were undertaken in reflection mode, under vacuum and at room temperature.

3 Results

Figure 1 illustrates the X-ray diffraction pattern of the composite after sintering. As shown the majority of HA decomposed to form β-tricalcium phosphate (β-$Ca_3(PO_4)_2$) during sintering with only residual levels of hydroxyapatite remaining. In addition to the mullite phase small amounts of alumina were also detected whilst there were negligible levels of gehlentie or CaO present as shown in Fig. 1. Previous studies showed that the 20% mullite composites exhibited superior mechanical properties compared to monolithic hydroxyapatite as reported by Nath et al. [33]. Fluorescence maps of samples explanted after 1 and 12 weeks are given in Figs. 2 and 3, respectively. The dimensions of the maps correspond to an area 800 μm long by 200 μm high and have a 5 μm resolution. The left hand side corresponds to the ceramic and the right hand side to the soft tissue region. A relatively sharp interface region exists between the ceramic and soft tissue for each of the elements (Al, Si, P and Ca) studied. The four elements were mapped simultaneously to ensure good registry. It is evident that there is a positive correlation between the concentration of Ca and P within the ceramic region (c.f. Figs. 2c with d, and 3c with d). This results from Ca and P being introduced in the form of hydroxyapatite (and the resultant tricalcium phosphate (TCP) phase present after sintering) and represents small non-uniformities in the sinter composite. The correlation between Ca and P is still present in the 12 week sample, confirming that the majority of the CaP phase remains intact within the ceramic over this period of time, this is consistent with the work of Nath et al. who reported limited resoprtion even after 12 weeks of implantation [11]. The limited resorption of TCP was attributed to the presence of the mullite phase at the grain boundary [11]. The correlation between Si and Al levels (c.f. Figs. 2a with b, and 3a with b) is less well defined. This is attributed in part to the lower concentrations and also because the mullite has an average grain size of only 2 μm after sintering which is smaller than the incident beam. Small non-uniformities in the composition of the ceramic composite exist despite mixing with a ball mill for 16 h. A single spot (~4 pixels) above background level is observed in the map of the 1-week sample; this is attributed to a small piece of debris resulting from the implant/explants procedure rather than leaching from the ceramic. No bright spots were seen in the 4- or 12-week samples.

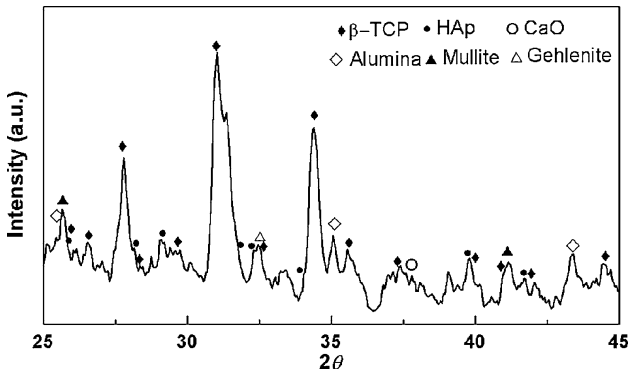

Fig. 1 X-ray diffraction pattern of the resultant CaP-Mullite ceramic after sintering at 1350 °C for 2 h

Figure 4 illustrates the intensity of the aluminium fluorescence for the 1- and 12-week samples. Figure 5 shows the line scan plot of the average fluorescence intensity for each of the four elements probed. As shown, the relative intensities of Ca and P fell at the ceramic interface by ~25 and 12% respectively for the sample after 12 weeks implantation. This may be expected since TCP is bioresorbable and the resulting precipitation of Ca and P into new bone is initially in the form of an amorphous calcium phosphate (ACP). This ACP is not fully densified and can contain between 15 and 20% of water [34]. The bulk ceramic contains TCP with a Ca/P ratio of 1.5, given the resultant Ca/P levels present at the interface region after 12 weeks of implantation, the Ca/P ratio at the interface is estimated to be ~1.77(5). ACP can take a wide range of compositions of the form of $Ca_xH_y(PO_4)_z.nH_2O$, where n = 3–4.5, and can consist of a Ca/P molar ratio between 1.0 and 2.2, thus the present Ca/P values are consistent with existing literature [34]. The Al intensity increases at the ceramic interface whilst remaining in the ceramic region. This is partly attributed to the lower concentrations of Ca and P present, thus reducing the sample self attenuation of the incident X-ray beam at the interface. Note at an incident energy of 4.1 keV, the X-ray intensity falls to 1/e of its initial intensity when penetrating 6 μm of TCP. Figures 4 and 5 illustrate the sharp interface between ceramic and tissue. The fluorescence intensity (and hence concentration) falls almost two orders of magnitude to the background level over a 35 μm interface region (7 data points each 5 μm wide). The interface region is sharper for Al and Si compared to Ca and P, as expected from the chemical durability of mullite and TCP and the precipitation process of ACP.

4 Discussion

During the sintering process the majority of HA decomposed to form β-tricalcium phosphate, $Ca_3(PO_4)_2$, as shown

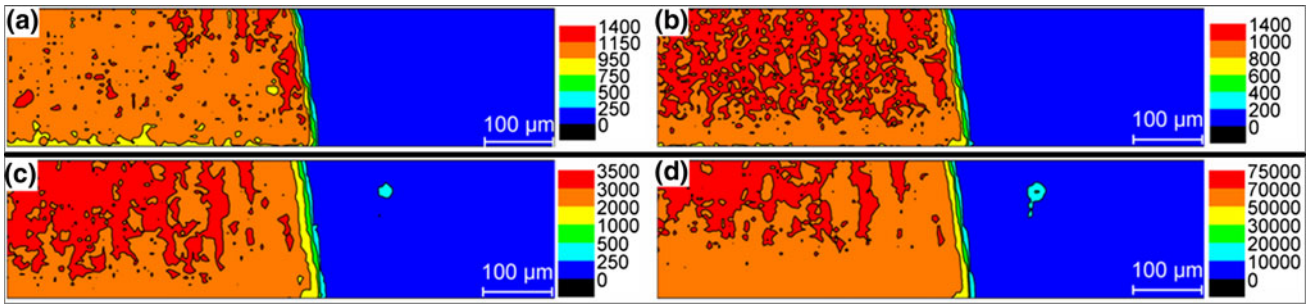

Fig. 2 Fluorescence maps for the 1 week sample. **a**, **b**, **c** and **d** represent Al, Si, P and Ca respectively. The intensity represents the fluorescence signal and is in arbitrary units. The dimensions of each map are 800 μm long by 200 μm wide. The high intensity region on the *left hand side* represents the ceramic whilst the low intensity region on the *right hand side* corresponds to soft tissue

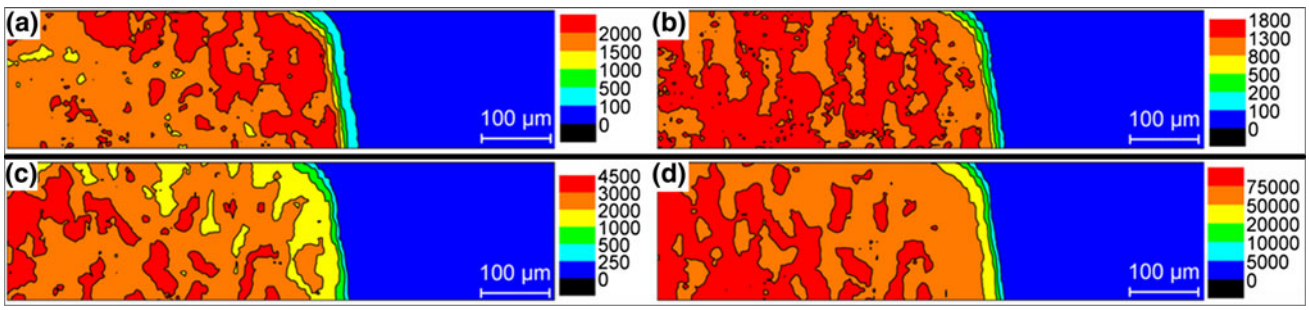

Fig. 3 Fluorescence maps for the 12 week sample. **a**, **b**, **c** and **d** represent Al, Si, P and Ca respectively. The intensity represents the fluorescence signal and is in arbitrary units. The dimensions of each map are 800 μm long by 200 μm wide. The high intensity region on the *left hand side* represents the ceramic whilst the low intensity region on the *right hand side* corresponds to soft tissue

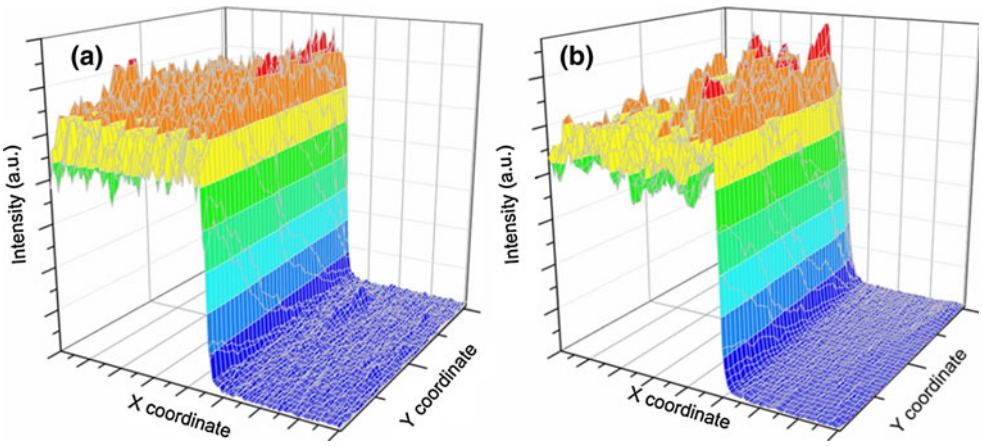

Fig. 4 Surface plot of the aluminium intensity for the 1 week (**a**) and 12 week (**b**) implanted sample

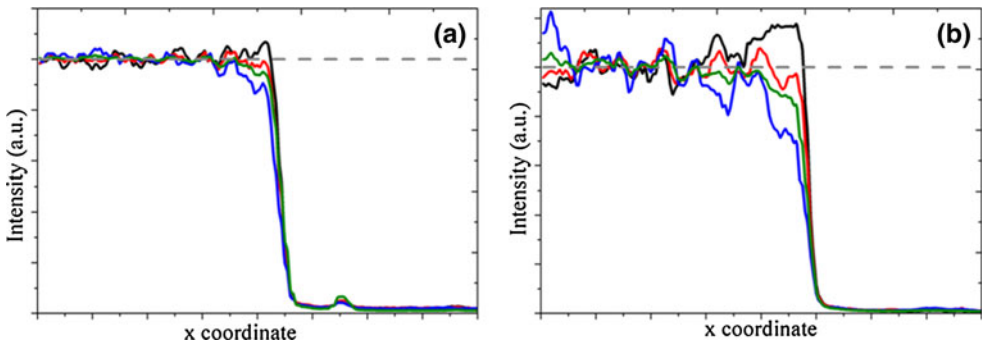

Fig. 5 Line plots illustrating the averaged y coordinate fluorescence intensity. The intensity level has been scaled such that the intensity inside the ceramic area oscillates around a common single value. **a** and **b** represent the 1 and 12 week samples respectively. The Al, Si, P and Ca are represented by the *solid black*, *red*, *blue* and *green lines* respectively. The *dashed grey curve* represents the normalised average intensity of the ceramic region

in Fig. 1. This is important since although HA is the mineral component found in teeth and bones it is also the most stable and least soluble form [35] and consequently not bioresorbable by osteoclasts [36]. However TCP is bioresorbable and osteoconductive [36, 37]. Previous studies investigating the ceramic/hard tissue (bone) interface have demonstrated that the CaP-20 wt% mullite composite is bioactive and stimulates new bone formation [11].

Aluminium was found to reside within ~35 μm of the ceramic–soft tissue interface. The exact role of aluminium within this interface region is difficult to fully interpret. Firstly, the surface of the implanted ceramic was not polished prior to implantation and may therefore have small surface irregularities which become significant at the 5 μm length scale. Secondly, the exact profile of the incident X-ray beam is not a square top-hat function. The spot size, characterised using knife edge scans through the focal are given as full width half maximum [32]. This might lead to a small artificial broadening of the interface. Critically, the interface region was not found to increase between the 1 and 12 week implanted samples. Furthermore, there were no detectable signs of aluminium leaching further into the surrounding soft tissue, beyond this interface region, thus indicating that Al remains localised in the ceramic or the ceramic interface. This might be expected in part given the chemical durability of these ceramics and the affinity of aluminium for phosphate species [15]. Note, previous studies conducting using radioactive ^{26}Al have shown that aluminium is preferentially absorbed into bone at levels ~100 times that observed in brain tissue [16]. It is therefore reasonable that aluminium introduced in the vicinity of bone would remain in close proximity to the implant site. However, from a clinical perspective it is still important that the concentrations of Al are directly measured in brain tissue and other organs to confirm our findings that the implant does not release potentially dangerous levels of Al.

In vitro dissolution of the CaP-20 wt% mullite composite has shown that significant quantities of Ca and P (~100 and 1,000 mg/L respectively) are released from the CaP phase of the sample when placed in simulated body fluid [12]. This ion release is essential for bioactivity and to enable the formation of new bone [11]. On the other hand alumina-silicates are known to be extremely chemically durable. Indeed, alumina-silicates are so insoluble under standard conditions that highly corrosive acids such as hydrofluoric acid are typically used for surface etching [38]. Importantly,

during the preparation of this composite the mullite phase remained distinct during the sintering process as shown in the fluorescence mapping, consequently the rate of dissolution of aluminium from the mullite phase does not increase significantly for the composite.

5 Conclusions

CaP-20 wt% mullite composites were successfully implanted into the long bones of healthy rabbits for up to 12 weeks. X-ray micro-fluorescence was shown to be a powerful technique capable of mapping simultaneously the distribution of Al, P, Si and Ca elements across the ceramic/soft tissue interface at a resolution of 5 μm. The mullite phase of the ceramic composite was found to be chemically durable under physiological conditions and the potential movement of aluminium was found to be restricted to a small interface region. This interface between the ceramic and the surrounding soft tissue was ~35 μm wide, within which the fluorescence intensity reduced by two orders of magnitude to the background level. The width of this interface did not increase for Al in the 12 week sample compared to the 1 week sample. Furthermore, there were no detectable signs of aluminium leaching further out (>35 μm) into the surrounding soft tissue areas. Previous studies on this composite have found no signs of inflammation and new bone formation to be present after 12 weeks of implantation [11]. It is therefore concluded that no significant quantities of aluminium leach from the CaP-20 wt% mullite samples beyond a small interface region over the 12 week implantation period and that the samples may offer a potential as a suitable bone replacement material for orthopaedic applications.

Acknowledgments The authors would like to thank R.J. Newport for helpful discussions and advice; they acknowledge a British Council Award (No 13973) as well as funding from the Department of Science and Technology, Government of India. This research was conducted under the framework of UK-India Education and Research Initiative (UKIERI) that facilitates the collaboration between IIT Kanpur and the University of Birmingham. The authors would like to thank the French National Synchrotron Facility, Soleil, for the allocation of beam-time.

References

1. Hench LL. Bioceramics: from concept to clinic. J Am Ceram Soc. 1991;74:1487–510.
2. Gautier S, Champion E, Assollant DB. Processing, microstructure and toughness of Al_2O_3 platelet-reinforced hydroxyapatite. J Euro Ceram Soc. 1997;17:1361–9.
3. Li J, Fartash B, Hermansson L. Hydroxyapatite—alumina composites and bone-bonding. Biomaterials. 1995;16:417–22.
4. Rao RR, Kannan TS. Synthesis and sintering of hydroxyapatite–zirconia composites. Mater Sci Eng C. 2002;20:187–93.
5. Silva VV, Lameiras FS, Domínguez RZ. Microstructural and mechanical study of zirconia-hydroxyapatite (ZH) composite ceramics for biomedical applications. Compos Sci Technol. 2001;61:301–10.
6. Gollera G, Demirkıran H, Oktar FN, Demirkesen E. Processing and characterization of bioglass reinforced hydroxyapatite composites. Ceram Inter. 2003;29:721–4.
7. Suchanek W, Yashima M, Kakihana M, Yoshimura M. Hydroxyapatite/hydroxyapatite-whisker composites without sintering additives: mechanical properties and microstructural evolution. J Am Ceram Soc. 1997;80:2805–13.
8. Kaye GWC, Laby TH. Table of physical and chemical constants. 15th ed. London and New York: Longman; 1986.
9. Erbe EM, Day DE. Chemical durability of Y_2O_3–Al_2O_3–SiO_2 glasses for the in vivo delivery of beta radiation. J Biomed Mater Res. 1993;27:1301–8.
10. Martin RA, Salmon PS, Carroll DL, Smith ME, Hannon AC. Structure and thermal properties of yttrium alumino-phosphate glasses. J Phys Condens Matter. 2008;20:115204.
11. Nath S, Basu B, Mohanty M, Mohanan PV. In vivo response of novel hydroxyapatite-mullite composites: results up to 12 weeks of implantation. J Biomed Mater Res B. 2009;90:547–57.
12. Priya A, Nath S, Basu B, Biswas K. In vitro dissolution of calcium phosphate-mullite composite in simulated body fluid. J Mater Sci Mater Med. 2010;21:1817–28.
13. Nath S, Raghunandan U, Basu B. Fretting wear behavior of calcium phosphate-mullite composites in dry and albumin-containing simulated body fluid conditions. J Mater Sci Mater Med. 2010;21:1151–61.
14. Yokel RA, McNamara PJ. Aluminium toxicokinetics: an updated mini review. Pharmacol Toxicol. 2001;88:159–67.
15. Williams RJP. What is wrong with aluminium?. The J.D. Birchall memorial lecture. J Inorg Biochem. 1999;76:81–8.
16. Priest ND. The biological behaviour and bioavailability of aluminium in man, with special reference to studies employing aluminium-26 as a tracer: review and study update. J Environ Monit. 2004;6:375–403.
17. Julka D, Gill KD. Altered calcium homeostasis: a possible mechanism of aluminium-induced neurotoxicity. Biochimica et biophysica acta. 1996;1315:47–54.
18. Carter DH, Sloan P, Brook IM, Hatton PV. Role of exchanged ions in the integration of ionomeric (glass polyalkenoate) bone substitutes. Biomaterials. 1997;18:459–66.
19. Devlin AJ, Hatton PV, Brook IM. Dependence of in vitro biocompatibility of ionomeric cements on ion release. J Mater Sci Mater Med. 1998;9:737–41.
20. Hantson PH, Mahieu P, Gersdorff M, Sindic CJM, Lauwerys R. Encephalopathy with seizures after use of aluminium-containing bone cement. Lancet. 1994;344:1647.
21. Renard JL, Felten D, Bequet D. Post-otoneurosurgery aluminium encephalopathy. Lancet. 1994;344:63–4.
22. Reushe E, Pilz P, Oberascher G, Linder B, Egensperger R, Gloeckner K, et al. Subacute fatal aluminium encephalopathy after reconstructive otoneurosurgery. Hum Pathol. 2001;32:1136–40.
23. Hurrell-Gillinghama K, Reaney IM, Brook I, Hatton PV. In vitro biocompatibility of a novel Fe_2O_3 based glass ionomer cement. J Dent. 2006;34:533–8.
24. Blades MC, Moore DP, Revell PA, Hill R. In vivo skeletal response and biomechanical assessment of two novel polyalkenoate cements following femoral implantation in the female New Zealand White rabbit. J Mater Sci Mater Med. 1998;9:701–6.
25. http://www.food.gov.uk/news/newsarchive/2008/jul/alu.

26. Joint FAO/WHO expert committee on food additives. Sixty-seventh meeting Rome, 20–29 June 2006. ftp://ftp.fao.org/ag/agn/jecfa/jecfa67_final.pdf.
27. Ljunggren KG, Lidums V, Sjogren B. Blood and urine levels of aluminium among workers exposed to aluminium flakes. Br J Ind Med. 1991;48:106–9.
28. Williams JW, et al. Biliary excretion of aluminium in aluminium osteodystrophy with liver disease. Ann Intern Med. 1986;104:782.
29. Flarend RE, Hem SL, White JL, Elmore D, Suckow MA, Rudy AC, Dandashli EA. In vivo absorption of aluminium containing vaccine adjuvants using 26Al. Vaccine. 1997;15:1314–8.
30. Santos MH, Oliveira M, Souza LPF, Mansur HS, Vasconcelos WL. Synthesis control and characterization of hydroxyapatite prepared by wet precipitation process. Mater Res. 2004;7:625–30.
31. Flank AM, et al. LUCIA, a microfocus soft XAS beamline. Nucl Instrum Methods Phys Res B. 2006;246:269–74.
32. Lagarde P, Flank AM, Vantelon D and Janousch M, Micro-Soft X-Ray Spectroscopy with the LUCIA Beamline. In AIP conference proceedings X-ray absorption fine structure—XAFS13: 13th international conference 2007;882:852–857.
33. Nath S, Biswas K, Wang K, Bordia RK, Basu B. Sintering, phase stability, and properties of calcium phosphate-mullite, composites. J Am Ceram Soc. 2010;93(6):1639–49.
34. Dorozhkin SV. Amorphous calcium (ortho)phosphates. Acta Biomater. 2010;6:4457–75.
35. Klein CPAT, de Blieck-Hogervorst JMA, Wolke JGC, de Groot K. Studies of the solubility of different calcium phosphate ceramic particles in vitro.
36. Yamada S, Heymann D, Bouler JM, Daculsi G. Osteoclastic resorption of calcium phosphate ceramics with different hydroxyapatite/β-tricalcium phosphate ratios. Biomaterials. 1997;18:1037–41.
37. Gatti AM, Zatfe D, Poli GP. Behaviour of tricalcium phosphate and hydroxyapatite granules in sheep bone defects. Biomaterials. 1990;11:513–7.
38. Takei T, Hayashi S, Yasumori A, Okada K. Pore structure and thermal stability of mesoporous mullite fibers prepared by crystallization and selective leaching of Al_2O_3–SiO_2 glass fibers. J Porous Mater. 1999;6:119–26.